

# First principles perspective on the microscopic model for $\text{Cs}_2\text{CuCl}_4$ and $\text{Cs}_2\text{CuBr}_4$

K Foyevtsova, Y Zhang, H O Jeschke and R Valentí

Institut für Theoretische Physik, Goethe-Universität Frankfurt, Max-von-Laue-Straße 1, 60438 Frankfurt am Main, Germany

E-mail: foyevtsova@itp.uni-frankfurt.de

**Abstract.** We investigate the microscopic model for the frustrated layered antiferromagnets  $\text{Cs}_2\text{CuCl}_4$  and  $\text{Cs}_2\text{CuBr}_4$  by performing *ab initio* density functional theory (DFT) calculations and with the help of the tight-binding method. The combination of both methods provide the relevant interaction paths in these materials, and we estimate the corresponding exchange constants. We find for  $\text{Cs}_2\text{CuCl}_4$  that the calculated ratio of the strongest in-plane exchange constants  $J'/J$  between the spin-1/2 Cu ions agrees well with neutron scattering experiments. The microscopic model based on the derived exchange constants is tested by comparing the magnetic susceptibilities obtained from exact diagonalization with experimental data. The electronic structure differences between  $\text{Cs}_2\text{CuCl}_4$  and  $\text{Cs}_2\text{CuBr}_4$  are also analyzed.

## 1. Introduction

The frustrated layered antiferromagnets  $\text{Cs}_2\text{CuCl}_4$  and  $\text{Cs}_2\text{CuBr}_4$  have recently attracted a lot of interest because of unconventional magnetic properties [1, 2, 3]. While in  $\text{Cs}_2\text{CuCl}_4$ , a magnetic field induced Bose-Einstein condensation (BEC) of magnons [3] and spin-fractionalization [2] have been observed,  $\text{Cs}_2\text{CuBr}_4$ , though being iso-structural to  $\text{Cs}_2\text{CuCl}_4$ , shows no sign of BEC. Instead, its field-dependent magnetization shows two plateaux [1].

Both compounds have been classified as two-dimensional systems, with an underlying anisotropic triangular lattice of spin-1/2  $\text{Cu}^{2+}$  ions (right panel of figure 1). The ratio of the two antiferromagnetic exchange constants in the triangular lattice,  $J'/J$  (see figure 1) has been found from neutron scattering experiments to be 0.34 for  $\text{Cs}_2\text{CuCl}_4$  [4] and 0.74 for  $\text{Cs}_2\text{CuBr}_4$  [1]. The interlayer couplings as well as the Dzyaloshinski-Moriya interaction also present in these systems are suggested to be an order of magnitude smaller than  $J$  and  $J'$ .

Yet, since extracting the exchange constants from the neutron scattering experiment data is based on the assumption of a suitable Hamiltonian, there is a need to support experimental findings with theoretical predictions. This motivated us to perform density functional theory calculations on  $\text{Cs}_2\text{CuCl}_4$  and  $\text{Cs}_2\text{CuBr}_4$  as presented in this work.

## 2. Computational details

We have performed density-functional calculations in the generalized gradient approximation (GGA) [5], using the full-potential linearized augmented plane wave (LAPW) method implemented in the WIEN2k code [6]. With  $RK_M = 7.0$  and 120  $k$ -points in the irreducible Brillouin zone, we obtained well-converged results for both  $\text{Cs}_2\text{CuCl}_4$  and  $\text{Cs}_2\text{CuBr}_4$ . For

$\text{Cs}_2\text{CuCl}_4$  we took the experimental room-temperature structure reported in [7], and for  $\text{Cs}_2\text{CuBr}_4$  we used the structure reported in [8].

### 3. Crystal structure

$\text{Cs}_2\text{CuCl}_4$  and  $\text{Cs}_2\text{CuBr}_4$  crystallize in the orthorhombic space group  $Pnma$  (see figure 1). The unit cell contains four formula units and has lattice parameters  $a = 9.769 \text{ \AA}$ ,  $b = 7.607 \text{ \AA}$  and  $c = 12.381 \text{ \AA}$  for  $\text{Cs}_2\text{CuCl}_4$  and  $a = 10.195 \text{ \AA}$ ,  $b = 7.965 \text{ \AA}$  and  $c = 12.936 \text{ \AA}$  for  $\text{Cs}_2\text{CuBr}_4$ . Each of the four equivalent  $\text{Cu}^{2+}$  ions is surrounded by four halogen ( $\text{Cl}^-$  or  $\text{Br}^-$ ) ions located at the vertices of a squeezed tetrahedron. The  $\text{CuCl}_4^{2-}/\text{CuBr}_4^{2-}$  complexes arranged in a two-dimensional triangular lattice form layers parallel to the  $bc$  plane separated along  $a$  by  $\text{Cs}^+$  ions. The most important superexchange pathways between Cu ions have been determined [4, 1] to be those within a  $\text{CuCl}_4^{2-}/\text{CuBr}_4^{2-}$  layer ( $J$  and  $J'$  in the right panel of figure 1). The magnetic interaction is mediated via halogen ions.

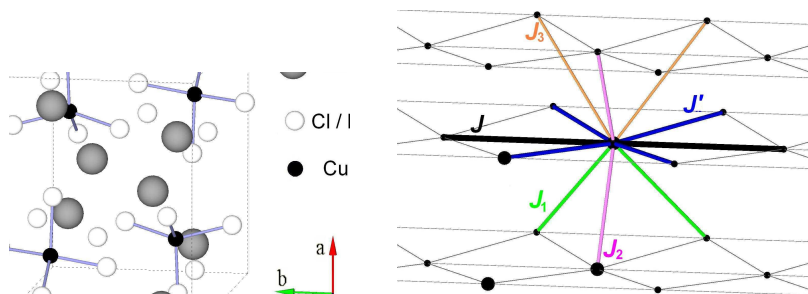


**Figure 1.** Left: Unit cell of  $\text{Cs}_2\text{CuBr}_4$  and  $\text{Cs}_2\text{CuCl}_4$ . Right: Lattice of magnetic Cu sites where the five most important interaction pathways are shown.

### 4. Electronic structure

In panels (a) and (b) of figure 2 we present the calculated bandstructures of  $\text{Cs}_2\text{CuCl}_4$  and  $\text{Cs}_2\text{CuBr}_4$ . Cu  $t_{2g}$  states that are hybridized via halogen  $p$  states lie in the range of energies between  $-0.6 \text{ eV}$  and  $0.1 \text{ eV}$ . The twelve bands originate from the three Cu  $t_{2g}$  orbitals which are split due the distorted tetrahedron crystal field of halogen ions. In  $\text{Cs}_2\text{CuCl}_4$ , the four partially unoccupied higher-energy Cu  $3d_{xy}$  bands are separated from the nearly degenerate Cu  $3d_{xz}$  and Cu  $3d_{yz}$  bands by a narrow gap. In  $\text{Cs}_2\text{CuBr}_4$ , the gap is absent. Out of these bandstructure features we conclude that the low-energy behavior of  $\text{Cs}_2\text{CuCl}_4$  can be described by a one-band model ( $d_{xy}$ ) while the three Cu  $t_{2g}$  band model is necessary for the description of  $\text{Cs}_2\text{CuBr}_4$ .

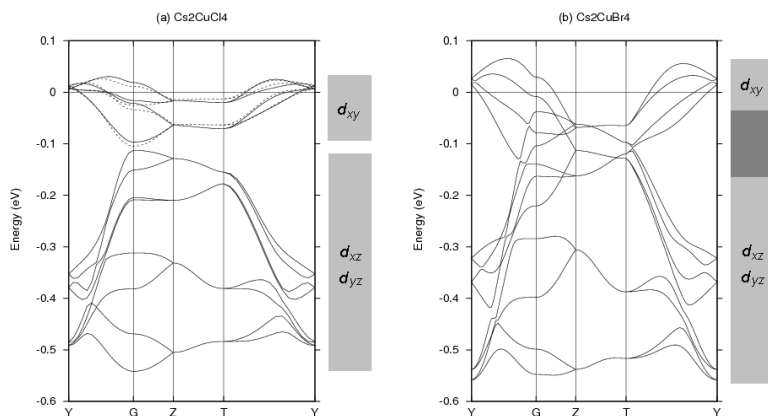


**Figure 2.** Bandstructure of  $\text{Cs}_2\text{CuCl}_4$  (a) and  $\text{Cs}_2\text{CuBr}_4$  (b). Dashed lines in (a) are the tight-binding fit.

Both  $\text{Cs}_2\text{CuCl}_4$  and  $\text{Cs}_2\text{CuBr}_4$  are Mott insulators. The fact that the GGA functional gives a metallic state is due to the insufficient treatment in this approach of electronic correlations.

Consideration of GGA+U provides the correct insulating behavior. Since we are interested in obtaining the effective hopping matrix elements between the Cu ions, we will consider in what follows the GGA exchange-correlation functional.

The Cu  $3d_{xy}$  bands of  $\text{Cs}_2\text{CuCl}_4$  are comparatively less dispersive than those of  $\text{Cs}_2\text{CuBr}_4$ . It is then to be expected that the hopping parameters between magnetic Cu ions in  $\text{Cs}_2\text{CuCl}_4$  will be smaller than in  $\text{Cs}_2\text{CuBr}_4$ . In  $\text{Cs}_2\text{CuCl}_4$ , the bands are almost flat in the  $k_x$ -direction, which indicates that layers of Cu ions (parallel to the  $bc$ -plane) are weakly coupled. Both observations are in agreement with experiment.

### 5. Calculation of exchange couplings for $\text{Cs}_2\text{CuCl}_4$

Based on the LAPW bandstructure (figure 2 (a)), we have calculated hopping integrals between magnetic Cu ions of  $\text{Cs}_2\text{CuCl}_4$  using the tight-binding (TB) method. We constructed a single-orbital TB Hamiltonian intended to describe the bands near the Fermi level, which are the Cu  $3d_{xy}$  bands in  $\text{Cs}_2\text{CuCl}_4$ . The hopping integrals  $t$  entering the Hamiltonian were varied until the best possible fit of the TB bands to the LAPW bands was achieved (dashed lines in figure 2 (a)). Application of the TB method for  $\text{Cs}_2\text{CuBr}_4$  is very involved since one needs to consider a three-orbital Hamiltonian to describe the overlap of the three Cu  $t_{2g}$  bands. The number of variational parameters of the three-band model Hamiltonian greatly increases due to all possible inter-orbital hoppings.

In table 1 we list the eight hopping integrals  $t$  that we included in the Hamiltonian for  $\text{Cs}_2\text{CuCl}_4$ . The interaction pathways corresponding to  $t$ ,  $t'$ ,  $t_1$ ,  $t_2$  and  $t_3$  are shown in figure 1 (labeled by the corresponding exchange constants  $J$ ).  $J = J^{\text{FM}} + J^{\text{AFM}}$  where  $J^{\text{FM}}$  is

**Table 1.** Calculated hopping integrals  $t_i$  with corresponding exchange constant ratios  $(J_i/J_{\text{max}}) = (t_i/t_{\text{max}})^2$  versus experimentally determined exchange constants  $J^{\text{exp}}$  for  $\text{Cs}_2\text{CuCl}_4$ .

Interaction paths ( $p$ )	$pJ$	$pJ'$	$pJ_1$	$pJ_2$	$pJ_3$	$pJ_4$	$pJ_5$	$pJ_6$
$t_i$ (meV)	-11.7	-6.75	4.20	-5.18	-8.39	-2.17	-4.11	-3.35
$(J_i/J_{\text{max}}) = (t_i/t_{\text{max}})^2$	1	0.336	0.131	0.197	0.516	0.033	0.123	0.074
$(J_i/J_{\text{max}})^{\text{exp}}$	1	0.342	—	0.045	—	—	—	—

the ferromagnetic component of the exchange while  $J^{\text{AFM}}$  describes the antiferromagnetic contributions to the total exchange constant.  $J_i^{\text{AFM}}$  can be estimated by applying perturbation theory on the Hubbard model as  $J_i^{\text{AFM}} = 4t_i^2/U$  where  $t_i$  are the hopping integrals and  $U$  is the on-site Coulomb repulsion. An alternative way of calculating  $J$  is by considering total energies of various magnetic configurations. In Ref. [9] we found by considering total energy differences that the ferromagnetic contributions are negligible for the strongest interactions, which allows us to compare the obtained  $J_i^{\text{AFM}}$  from  $t_i$  with the  $J_i$  obtained from experimental data. In table 1 we present the calculated (second row) and experimentally fitted (third row) ratios  $J_i/J_{\text{max}}$ , which are independent of  $U$ . We observe that the calculated in-plane exchange ratio  $J'/J = 0.336$  agrees well with the experimentally fitted 0.342. At the same time, we observe that the antiferromagnetic contribution of the interlayer exchange constants  $J_1$ ,  $J_2$  and  $J_3$  is also considerable, which implies a non-negligible three dimensional contribution of the exchange interactions in  $\text{Cs}_2\text{CuCl}_4$ .

The magnetic susceptibility of a Heisenberg Hamiltonian for  $\text{Cs}_2\text{CuCl}_4$  based on exchange couplings from our DFT calculations was calculated with the exact diagonalization method (the Hamiltonian of a 16-site system was diagonalized with periodic boundary conditions). Two

models were investigated: one including  $J$  and  $J'$  only and the other including  $J$ ,  $J'$  and the largest interlayer coupling  $J_3$ . In figure 3 we present the results together with experimental data. The susceptibility plot is rescaled in a way that only relative values of  $J$ 's play a role [10].

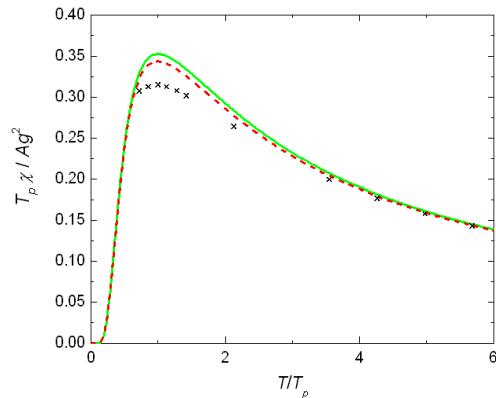


**Figure 3.** Susceptibility of  $\text{Cs}_2\text{CuCl}_4$  vs. temperature in units of the peak temperature  $T_p$ . Green solid line: DFT-based model with  $J$  and  $J'$ ; red dashed line: DFT-based model with  $J$ ,  $J'$  and  $J_3$ ; crosses: experimental data [11]. The susceptibility is scaled as  $T_p\chi/Ag^2$  with  $A = N_A\mu_B^2/4k = 0.0938$  cgs units and a  $g$  factor of  $g = 2.17$ .

We observe that inclusion of the interlayer coupling  $J_3$  has very little effect on the susceptibility and therefore other measurements like neutron scattering along the direction perpendicular to the  $bc$  plane are needed to investigate such possible interlayer couplings. We note that the less than perfect agreement of our exact diagonalization calculations with experiment is due to finite size effects[10].

In summary, we presented electronic structure calculations of  $\text{Cs}_2\text{CuCl}_4$  and  $\text{Cs}_2\text{CuBr}_4$ . While  $\text{Cs}_2\text{CuCl}_4$  can be well described by a single-band model with important  $J$ ,  $J'$  intralayer interactions and non-negligible interlayer coupling, a three-band model is needed for  $\text{Cs}_2\text{CuBr}_4$  due to the strong involvement of all Cu  $t_{2g}$  bands near the Fermi surface. We found that the magnetic susceptibility for  $\text{Cs}_2\text{CuCl}_4$  is not drastically changed by the inclusion of interlayer couplings in the model and therefore alternative measurements have to be considered to investigate the interlayer couplings in this material.

### Acknowledgments

We gratefully acknowledge support from the Deutsche Forschungsgemeinschaft via SFB/TRR 49 and Emmy Noether programs.

### References

- [1] Ono T *et al* 2005 *Prog. Theor. Phys. Suppl.* **159** 217-21
- [2] Coldea R, Tennant D A, Tsvelik A M, Tylczynski Z 2001 *Phys. Rev. Lett.* **86** 1335-8
- [3] Radu T, Wilhelm H, Yushankhai V, Kovrizhin D, Coldea R, Tylczynski Z, Lühmann T, Steglich F 2005 *Phys. Rev. Lett.* **95** 127202-1-4
- [4] Coldea R, Tennant D A, Habicht K, Smeibidl P, Wolters C, Tylczynski Z 2002 *Phys. Rev. Lett.* **88** 137203-1-4
- [5] Perdew J P, Burke K and Ernzerhof M 1996 *Phys. Rev. Lett.* **77** 3865-8
- [6] Blaha P, Schwarz K, Madsen G K H, Kvasnicka D and Luitz J 2001 *WIEN2k, An Augmented Plane Wave + Local Orbitals Program for Calculating Crystal Properties* (Karlheinz Schwarz, Techn. Universität Wien, Austria) ISBN 3-9501031-1-2.
- [7] Bailleul S, Svoronos D, Porcher P and Tomas A 1991 *Comptes Rendus Hebdomadaires des Seances de l'Academie des Sciences* **313** 1149-53
- [8] Morosin B and Lingafelter E C 1960 *Acta Cryst.* **13** 807-9
- [9] Foyevtsova K, Zhang Y, Jeschke H O, Valentí R (unpublished)
- [10] Zheng W, Singh R R P, McKenzie R H, Coldea R 2005 *Phys. Rev. B* **71** 134422-1-12
- [11] Tokiwa Y, Radu T, Coldea R, Wilhelm H, Tylczynski Z, Steglich F 2006 *Phys Rev B* **73** 134414-1-7